

Aminopyrimidine-Based Donor–Acceptor Chromophores: Push–Pull versus Aromatic Behaviour

Alejandro Ortíz,^[a,b] Braulio Insuasty,^{*,[a]} M. Rosario Torres,^[c] M. Ángeles Herranz,^[b] Nazario Martín,^{*,[b]} Rafael Viruela,^[d] and Enrique Ortí^{*,[d]}

Keywords: 2-Aminopyrimidines / Push–pull / Aromaticity / Nonplanar

Novel 2-aminopyrimidines substituted with two electron-donor dialkylamino groups and either one dicyanovinyl (**4a–d**) or one tricyanovinyl (**7a–d**) electron-acceptor group have been synthesized, and the balance between their push–pull character and their aromatic behaviour has been studied by experimental (spectroscopic, electrochemical and X-ray analysis) and theoretical (DFT/B3LYP/6-31G**) methods. Calculations reveal that the push–pull character is energetically favoured with respect to the preservation of the aromaticity of the pyrimidine ring. X-ray analysis of **7a** confirms the theoretical predictions and reveals a strong distortion from planarity due to the steric interaction between the tricyanovi-

nyl group and the adjacent dialkylamino moieties. In contrast with what would normally be expected for push–pull compounds, the visible-region absorption bands of **4a–d** and **7a–d** are associated with π – π^* electronic transitions and not with intramolecular charge-transfer absorptions. In each compound, both the HOMO and the LUMO are spread over the whole molecule and are not located on the donor and acceptor moieties, respectively, as is the case for typical push–pull chromophores.

(© Wiley-VCH Verlag GmbH & Co. KGaA, 69451 Weinheim, Germany, 2008)

Introduction

The concept of aromaticity has fascinated chemists over recent decades, and despite the great effort and resources consumed, there is currently no universally accepted definition of what aromaticity is or how it should be measured.^[1] Among the different criteria employed to define a molecule as an aromatic system, planarity is one of the most commonly used. However, a wide variety of nonplanar aromatic systems – in which the distortion from planarity can occur through twisting (helicenes), pyramidalization (fullerenes) or bending (cyclophanes) – are known. These and many other aspects (e.g., Möbius aromaticity) make aromaticity a still open and intriguing topic in chemistry.^[2]

Aminopyrimidines represent an important type of aromatic heterocyclic systems used in a wide variety of different fields. They have outstanding biological implications

as constituents of nucleotides and DNA, where the planarity of the ring has been recognized as an important factor that influences the molecular structure and the physical properties since it determines the π – π interactions within the heterocyclic framework.^[3] More recently, aminopyrimidine derivatives have been used in materials science for the preparation of supramolecular hydrogen-bonded systems based on oligo(*p*-phenylenevinylene) polymers and 2-ureido-4(1*H*)-pyrimidinone units,^[4] and also to obtain new supramolecular electrolytes for use in dye-sensitized solar cells.^[5] Other remarkable recent examples are the hierarchical self-assembly of all-organic photovoltaic devices achieved through the use of tetraaminopyrimidines^[6] and the design of calamitic/discotic cross-over mononuclear *ortho*-metallated mesogens formed from rod-like phenylpyrimidines.^[7]

Organic materials are known to be an excellent choice for use in nonlinear optical applications, and a wide variety of chromophores involving carbocyclic and heterocyclic systems have been used during the last twenty years.^[8] Helical pyridine-pyrimidine oligomers have shown remarkable nonlinear optical responses after the introduction of electron donor groups onto the pyrimidine ring. Furthermore, regular distributions of the donor groups around the helices enable the design of supramolecular structures showing dipolar, octupolar or Λ -shaped nonlinear optical properties.^[9]

These recent findings show the attraction of achieving a better knowledge of pyrimidine-based push–pull systems. In this regard, much less is known about aminopyrimidines

[a] Departamento de Química Orgánica, Facultad de Ciencias, Universidad del Valle, 25360 Cali, Colombia

E-mail: Braulio.insuasty@gmail.com

[b] Departamento de Química Orgánica, Facultad de Química, Universidad Complutense, 28040 Madrid, Spain

E-mail: nazmar@quim.ucm.es

[c] Centro de Asistencia a la Investigación de Rayos-X, Facultad de Química, Universidad Complutense, 28040 Madrid, Spain

[d] Institut de Ciència Molecular, Universitat de València, 46980 Paterna, Spain

E-mail: enrique.ortí@uv.es

bearing strong electron-acceptor groups, able to act as efficient push-pull systems. However, the aromatic character of the pyrimidine ring can be strongly modified by the presence of donor and acceptor moieties covalently connected through the nitrogen-containing ring.

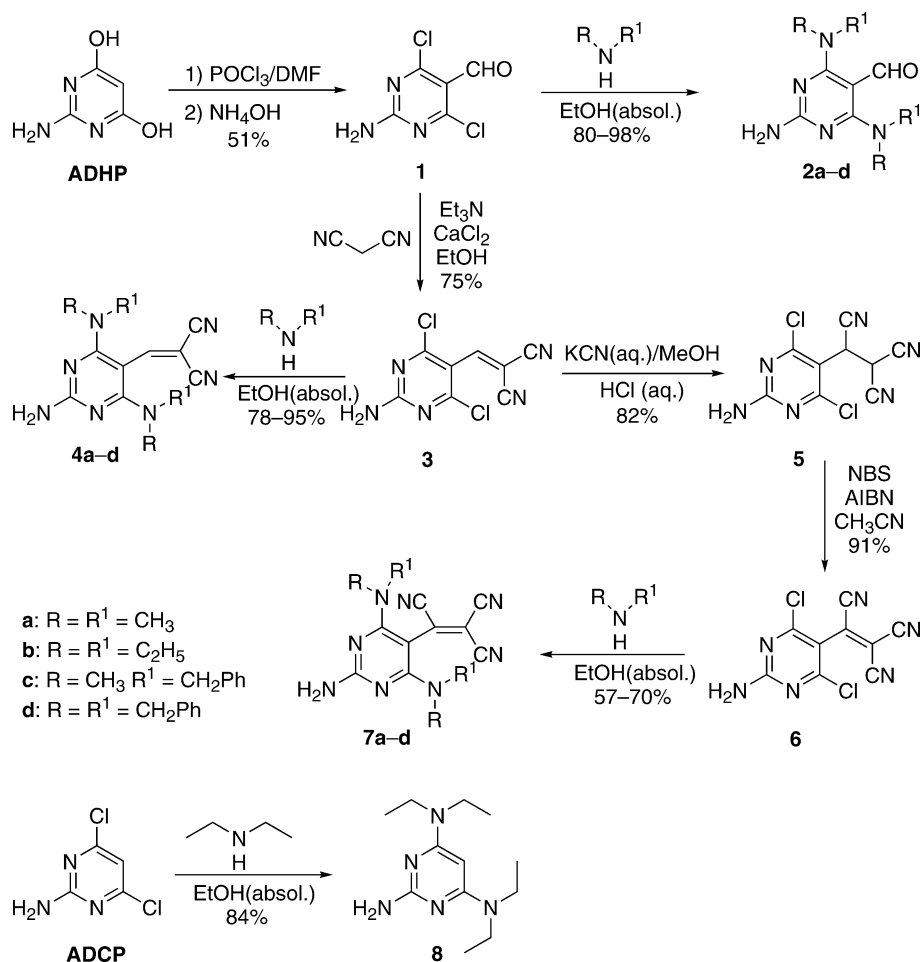
In this work we report on the preparation of new and remarkable push-pull aminopyrimidine derivatives bearing two strong electron-donor dialkylamino groups *ortho* either to an electron-acceptor dicyanovinyl group (**4a-d**; Scheme 1) or to a stronger electron-acceptor tricyanovinyl moiety (**7a-d**). Our main goal is to investigate how the presence of push-pull groups influences the aromatic character of the pyrimidine ring by modifying the electronic structure. Furthermore, in our case the presence of bulky groups such as tricyanovinyl and dialkylamino moieties might also play an important role by significantly distorting the geometry of the molecule. Therefore, in order to determine the electronic and geometrical properties of novel compounds **7a-d**, a thorough structural study has been carried out by means of spectroscopic techniques and X-ray diffraction for **7a**. Moreover, the redox properties of the new molecules in solution have been determined by cyclic voltammetry. A theoretical B3LYP/6-31G** study on the geometries and the electronic properties of the push-pull pyrimidine deriva-

tives complements this work. This theoretical approach has been successfully used in a recent study of the structural, electronic and electrochemical properties of pyridine-bridged push-pull compounds.^[10]

Results and Discussion

Synthesis and Characterization

The preparation of the novel push-pull compounds **4a-d** and **7a-d** was carried out in a multistep synthetic procedure from commercially available 2-amino-4,6-dihydroxypyrimidine (ADHP) as shown in Scheme 1. Pyrimidine derivative **1** was prepared by Vilsmeier formylation of ADHP as previously reported in the literature.^[11] Compounds **2a-d** and **3** were prepared from **1** in very good yields by treatment with the appropriate secondary amines in ethanol (**2a-d**) or by Knoevenagel condensation under basic conditions (**3**). From compound **3**, further treatment with secondary amines under the same standard conditions in alcoholic medium afforded push-pull compounds **4a-d** as stable yellow crystalline solids in very good yields.



Scheme 1. Synthesis of the push-pull aminopyrimidine derivatives.

Compounds **7a–d** were prepared from compound **3** in three steps, by treatment with potassium cyanide to form the tricyanoethane derivative **5** and further oxidation with NBS in the presence of azobis(isobutyronitrile) (AIBN) to provide the tricyanovinyl-containing compound **6** in 91% yield. Finally, treatment of **6** with the appropriate secondary amines in dry ethanol at reflux for 15–20 minutes afforded compounds **7a–d** in good yields (57–70%). Purification of the novel compounds was accomplished by column chromatography in silica gel, with CH₂Cl₂/CH₃OH (20:1) as the eluent. HPLC analyses [Cosmosil Buckyprep, CH₂Cl₂/CH₃OH (80:20)] revealed that these compounds were obtained in high purity (>99%). Finally, reference compound **8** was prepared in one synthetic step from 2-amino-4,6-dichloropyrimidine (ADCP) in 84% yield by treatment with diethylamine.

All the new synthesized compounds were unambiguously characterized by analytical and spectroscopic techniques. The low hydrogen contents in the new molecules give rise to relatively simple FTIR, ¹H NMR, ¹³C NMR and MS spectra, which confirm the proposed structures (see Exp. Sect.). The presence of the cyano groups provides some insight into the electronic and structural features. Compound **5** exhibits a band at 2258 cm⁻¹ in its FTIR spectrum, which indicates nonconjugated aliphatic nitriles. This stretching vibration mode appears at a lower value (2231 cm⁻¹) in compound **3**, due to the conjugation of the nitrile groups. In compounds **4a–d**, each bearing two strongly electron-releasing dialkylamino groups, the cyano stretching band shifts to lower values (2192–2204 cm⁻¹), thus suggesting an intramolecular charge transfer from the dialkylamino groups to the dicyanovinyl moiety. Previous studies on TCNQ (tetracyano-*p*-quinodimethane) salts have shown a linear relationship between the vibrational frequencies of the cyano groups and the degree of charge transfer (*Z*); the nitrile stretching for TCNQ thus ranges from 2227 cm⁻¹ for the neutral molecule (*Z* = 0) to 2183 cm⁻¹ for the potassium salt (*Z* = 1).^[12–16] In agreement with this observation, compounds **7a–d**, each bearing a stronger electron-acceptor tricyanovinyl unit, exhibit the lowest stretching vibrations, which now appear as two very intense and sharp bands (**7a**: 2196 and 2177 cm⁻¹). In contrast with the push–pull compounds **7a–d**, compound **6**, in which the dialkylamino groups are absent, only shows a band at 2199 cm⁻¹.

Density functional theory (DFT) calculations performed at the B3LYP/6-31G** level for the reference compounds **3**, **4a** and **7a** confirm the push–pull character predicted for derivatives **4** and **7**. For compound **3**, the C(CN)₂ group accumulates a total charge of –0.23 e and the CN bonds have a length of 1.163 Å. On passing to **4a**, the total charge of the C(CN)₂ group increases to –0.45 e, due to the charge transfer from the dialkylamino groups, and the CN bonds slightly lengthen to 1.166 Å. The softening of the CN bonds explains the shift to lower frequencies observed for the CN stretching bands in compounds **4**. The total charge calculated for the tricyanovinyl group of **7a** (–0.44 e) indicates a degree of charge transfer similar to that observed in **4a**. The charge is mainly accumulated on the C(CN)₂ group, which

now has CN bond lengths of 1.166 and 1.167 Å. Atomic charges were calculated by the natural population analysis (NPA) approach.

Molecular and Crystal Structure

In order to gain a better understanding of these new systems, we determined the X-ray structure of compound **7a**. A suitable crystal was obtained by crystallization from CH₂Cl₂/CH₃OH. Figure 1 shows an ORTEP view (40% probability) of the molecular structure, including the atomic numbering.^[17] Selected bond distances are collected in Table 1.

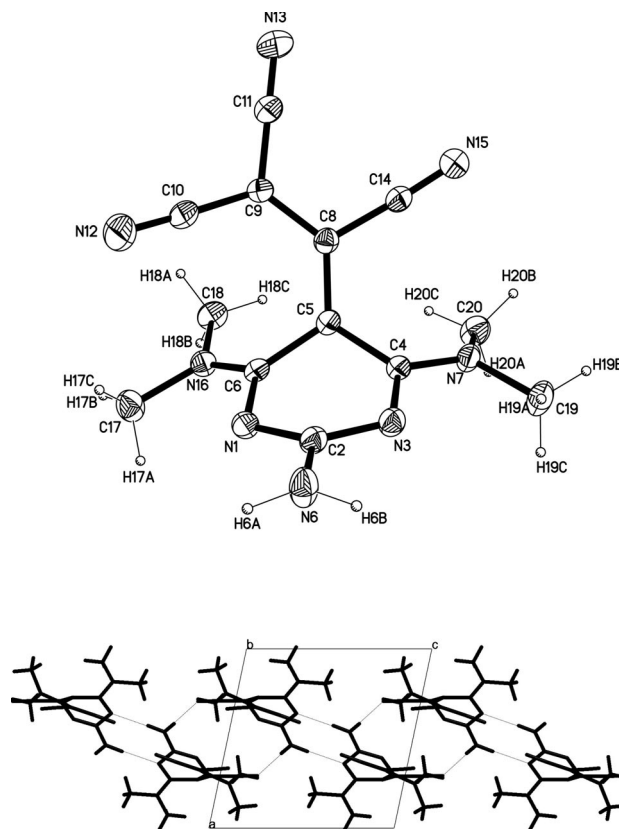


Figure 1. X-ray crystal structure of **7a**.

The pyrimidine ring in **7a** has a highly distorted structure. The C(5) atom, to which the tricyanovinyl group is attached, protrudes out of the plane of the ring and forms an angle of 30.5° with the average plane defined by the rest of the atoms forming the ring. The distortion from planarity is accompanied by a lengthening of the C(5)–C(4) and C(5)–C(6) bonds, which have lengths of 1.474(3) and 1.462(3) Å, respectively, much longer than those reported for the corresponding bonds in unsubstituted pyrimidine (1.393 Å).^[18] The bond lengths measured for the C–N bonds forming the ring (1.33–1.35 Å) are similar to those obtained for pyrimidine (1.340 Å).^[18] These results suggest that the pyrimidine ring in compound **7a** has partially lost its aromatic character.

Table 1. Experimentally determined X-ray and theoretical B3LYP/6-31G** values for selected bond lengths [Å] in neutral **7a** and in its oxidized (**7a⁺**) and reduced (**7a⁻** and **7a²⁻**) species.

| Bond | X-ray | 7a ^[a] | 7a⁺ ^[a] | 7a⁻ ^[a] | 7a²⁻ ^[a] | 7a²⁻ ^[a,b] |
|-------------|----------|--------------------------|--------------------------------------|--------------------------------------|---------------------------------------|---|
| C(2)–N(3) | 1.345(3) | 1.349 | 1.356 | 1.331 | 1.329 | 1.325 |
| C(2)–N(6) | 1.329(3) | 1.350 | 1.332 | 1.389 | 1.430 | 1.417 |
| C(2)–N(1) | 1.354(3) | 1.341 | 1.356 | 1.331 | 1.330 | 1.325 |
| C(4)–N(7) | 1.328(3) | 1.359 | 1.332 | 1.380 | 1.415 | 1.392 |
| C(4)–N(3) | 1.331(3) | 1.332 | 1.325 | 1.353 | 1.346 | 1.364 |
| C(4)–C(5) | 1.474(3) | 1.465 | 1.501 | 1.426 | 1.444 | 1.428 |
| C(5)–C(8) | 1.390(3) | 1.427 | 1.398 | 1.496 | 1.445 | 1.500 |
| C(5)–C(6) | 1.462(3) | 1.463 | 1.500 | 1.426 | 1.450 | 1.428 |
| C(6)–N(1) | 1.332(3) | 1.337 | 1.325 | 1.353 | 1.346 | 1.364 |
| C(6)–N(16) | 1.336(3) | 1.351 | 1.333 | 1.380 | 1.406 | 1.392 |
| C(8)–C(9) | 1.417(3) | 1.411 | 1.438 | 1.443 | 1.509 | 1.503 |
| C(8)–C(14) | 1.441(4) | 1.442 | 1.440 | 1.400 | 1.415 | 1.382 |
| C(9)–C(10) | 1.420(4) | 1.422 | 1.417 | 1.414 | 1.406 | 1.406 |
| C(9)–C(11) | 1.420(4) | 1.426 | 1.416 | 1.415 | 1.403 | 1.406 |
| C(10)–N(12) | 1.144(3) | 1.167 | 1.167 | 1.173 | 1.181 | 1.184 |
| C(11)–N(13) | 1.143(4) | 1.166 | 1.168 | 1.173 | 1.183 | 1.184 |
| C(14)–N(15) | 1.141(3) | 1.163 | 1.162 | 1.178 | 1.180 | 1.192 |
| C(17)–N(16) | 1.461(3) | 1.463 | 1.470 | 1.452 | 1.442 | 1.453 |
| C(18)–N(16) | 1.461(3) | 1.455 | 1.463 | 1.456 | 1.451 | 1.454 |
| C(19)–N(7) | 1.465(3) | 1.461 | 1.471 | 1.452 | 1.442 | 1.453 |
| C(20)–N(7) | 1.456(3) | 1.462 | 1.465 | 1.456 | 1.453 | 1.454 |

[a] Theoretical values calculated for the most stable conformations. [b] Values calculated for the perpendicular conformation depicted in part b of Figure 6.

In order to investigate the factors determining the molecular structure of **7a**, the geometry of this molecule was theoretically optimized, starting from different geometrical conformations. B3LYP/6-31G** calculations found four minima in the potential energy surface of **7a**.^[19] The most stable conformation is depicted in Figure 2 (a) and clearly corresponds to the X-ray structure shown in Figure 1. The second conformation sketched in Figure 2 (b) is calculated to be 1.59 kcal mol⁻¹ higher in energy. It corresponds to a structure in which the pyrimidine ring is almost planar, the tricyanovinyl group is rotated around the C(5)–C(8) bond by -49.8° [C(6)–C(5)–C(8)–C(9)], and the dimethylamino groups are twisted in opposite directions with respect to the pyrimidine plane to avoid steric interactions with the tricyanovinyl unit.

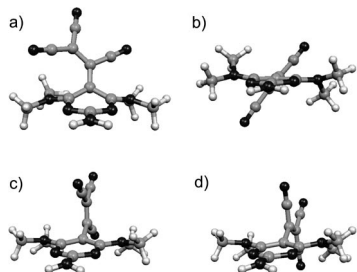


Figure 2. Minimum-energy conformations calculated for **7a** at the B3LYP/6-31G** level.

The two other minimum-energy structures (Figure 2, parts c and d) are perpendicular conformations in which the pyrimidine ring preserves its planarity and the tricyanovinyl group lies almost orthogonal to the ring. These conformations are calculated to be higher in energy than that in Fig-

ure 2 (a) by 5.02 and 7.10 kcal mol⁻¹, respectively. Higher level B3LYP calculations performed using the more extended 6-311+G** basis set predict very similar energy differences (1.40, 4.70 and 6.81 kcal mol⁻¹, respectively) with respect to the nonplanar conformation.

The theoretical results thus confirm the nonplanar structure obtained from X-ray diffraction as the most stable molecular conformation. C(5) is predicted to be “folded up” along the C(4)–C(6) axis by an angle of 26.0°, and the C(5)–C(4) and C(5)–C(6) bonds have lengths of 1.463 and 1.465 Å, respectively. These values are in good accord with those measured experimentally [30.5°, 1.474(3) Å and 1.462(3) Å].

Diederich et al. have recently synthesized a family of donor–acceptor compounds containing the closely related electron-acceptor 1,1,4,4-tetracyanobutadiene group.^[20] These compounds are also highly distorted from planarity. However, distortion mainly occurs by rotation around the central single bond of the tetracyanobutadiene unit and the aromatic rings preserve their planarity.

The distortion of **7a** from planarity is clearly due to the steric interaction between the tricyanovinyl unit and the neighbouring dimethylamino groups. Through the pushing up of the tricyanovinyl group, the interatomic distances between the nitrile atoms and the CH₃ hydrogens are in the range of 2.6–3.1 Å both in the X-ray and in the theoretical structures. The question to answer is why the molecule prefers to lose its planarity, and thereby the aromaticity of the pyrimidine ring, to alleviate those interactions instead of adopting a twisted conformation. Rotation of the tricyanovinyl group around C(5)–C(8) allows the pyrimidine ring to preserve its planarity, but disrupts the conjugation between the electron-acceptor group and the ring. However, the loss of conjugation has a more important destabilizing effect because it limits the charge transfer to the electron-acceptor group. In the perpendicular conformations sketched in Figure 2 (c and d), the tricyanovinyl group has a total charge of -0.15 e, in comparison with the charge of -0.44 e it has in the more stable nonplanar structure of Figure 2 (a). In the twisted conformation of Figure 2 (b), the charge accumulated by the tricyanovinyl group has an intermediate value of -0.29 e. Therefore, the push–pull character of the molecule is energetically favoured with respect to the preservation of the aromaticity of the pyrimidine ring. The energy difference between the nonplanar structure and the other three conformations indeed increases to 6.30 for the twisted structure and to 12.31 and 14.00 kcal mol⁻¹ for the perpendicular structures, when they are optimized in the presence of the solvent (CH₃CN). The solvent stabilizes the nonplanar structure because it promotes the charge transfer to the electron-acceptor tricyanovinyl group, which has a charge of -0.61 e in CH₃CN.

The molecular structures of compounds **2a**, **3** and **4a** were also optimized at the B3LYP/6-31G** level. Molecules **2a** and **4a**, bearing dimethylamino groups, display minimum-energy conformations similar to the nonplanar conformation obtained for **7a** (Figure 1 and 2, a). C(5) is “folded up” along the C(4)–C(6) axis, by angles of 14.2° for

2a and 20.6° for **4a**. In contrast, molecule **3**, in which the dimethylamino groups are absent, prefers to preserve the planarity of the pyrimidine ring and rotates the electron-acceptor group around the C(5)–C(8) bond by 52.7°. The different conformation adopted by **3** is attributed to the weaker push–pull character of this molecule.

Figure 1 shows that compound **7a** presents two intermolecular hydrogen bonds, giving rise to the formation of dimers (Table 2). Each molecule is linked to its centrosymmetric counterpart through the N6–H6A···N1B ($-x + 1, -y, -z + 1$) bond. The dimers thus formed are arranged in chains through the formation of a second hydrogen bond: N6–H6B···N1A ($-x + 1, -y, -z$). These chains of dimers are parallel to the “*b*” axis (see Figure 1). The dimer was fully optimized at the B3LYP/6-31G** level using C_i symmetry restrictions. Calculations correctly reproduce the hydrogen bond lengths (2.09 Å compared with the X-ray value of 2.12 Å) and predict an association energy of 8.25 kcal mol⁻¹ for the dimer.

Table 2. Hydrogen bond geometrical parameters for **7a** [Å and degrees].

| D–H···A | <i>d</i> (D–H) | <i>d</i> (H···A) | <i>d</i> (D···A) | <(DHA) |
|--------------------|----------------|------------------|------------------|--------|
| N(6)–H(6A)···N(1) | 0.96 | 2.12 | 3.066(3) | 170.4 |
| N(6)–H(6B)···N(15) | 0.97 | 2.19 | 3.149(4) | 170.6 |

Electronic Characterization

The λ_{\max} values for the electronic spectra of the final compounds **7a–d**, as well as those of some relevant intermediates for purposes of comparison, are collected in Table 3. The UV/Vis spectra registered in acetonitrile for the representative compounds **2a**, **4a** and **7a** are displayed in Figure 3. In contrast with the starting compounds **2a–d** and **3**, which absorb only in the UV region, the push–pull compounds **4a–d** and **7a–d** exhibit intense absorption bands in the visible region, which are responsible for the colour observed in these compounds. Compounds **4a–d** each show a broad absorption around 415 nm, which in principle can reasonably be assigned to an intramolecular charge transfer from the dialkylamino groups to the electron-accepting dicyanovinyl unit through the pyrimidine ring. Substitution of the dicyanovinylene group in **4a–d** by the stronger electron-acceptor tricyanovinylene group in **7a–d** results in a bathochromic shift of the absorption bands, which now appear around 460 nm.

Figure 4 shows the atomic orbital (AO) composition of the highest-occupied and lowest-unoccupied molecular orbitals (HOMO and LUMO) of **7a**. Although the LUMO shows a larger contribution on the tricyanovinylene group, both the HOMO and the LUMO are spread over the whole molecule. This contrasts with what is commonly found for push–pull systems, in which the HOMOs are usually mainly located over the donor parts of the molecules and the LUMOs mostly lie on the acceptors. Similar molecular orbital topologies are found for compounds **2a** and **4a**. The HOMO–LUMO energy gaps decrease on passing from **2a**

Table 3. Oxidation and reduction peak potentials (CH₃CN, in V vs. Ag/AgNO₃) and λ_{\max} values (CH₃CN in nm) for compounds **2a–d**, **3**, **4a–d**, **7a–d** and **8**.

| | E_{ox}^1 [a] | E_{red}^1 [b] | E_{red}^2 [b] | λ_{\max} ($\epsilon \times 10^{-4}$ cm L mol ⁻¹) |
|-----------|-----------------------|------------------------|------------------------|---|
| 8 | +0.871 | | | 289 (1.60) |
| 2a | +0.989 | | | 299 (1.04) |
| 2b | +0.930 | | | 302 (1.21) |
| 2c | +1.060 | | | 303 (1.32) |
| 2d | +1.033 | | | 299 (1.19) |
| 3 | | -1.289 | -1.842 | 335 (1.23) |
| 4a | +0.894 | | -1.975 | 411 (4.46) |
| 4b | +0.900 | | -1.964 | 417 (1.69) |
| 4c | +0.942 | | -1.890 | 413 (3.89) |
| 4d | +1.060 | | -1.831 | 417 (7.31) |
| 7a | +1.108 | -1.155 | -1.946 | 454 (13.9) |
| 7b | +1.107 | -1.122 | -2.119 | 460 (1.69) |
| 7c | +1.180 | -1.113 | -1.904 | 460 (7.24) |
| 7d | +1.190 | -1.114 | -1.854 | 465 (27.3) |

[a] Anodic peak potentials are reported. [b] Cathodic peak potentials are reported.

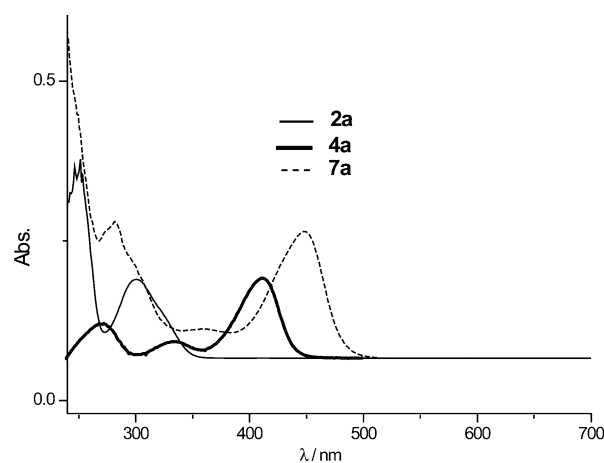


Figure 3. UV/Vis absorption spectra of compounds **2a**, **4a** and **7a** in CH₃CN.

(4.88 eV) to **4a** (3.74 eV) and from **4a** to **7a** (3.24 eV). This narrowing is due to the progressive stabilization of the LUMO (−0.66, −1.83, and −2.60 eV, respectively) as the electron-acceptor group becomes stronger.

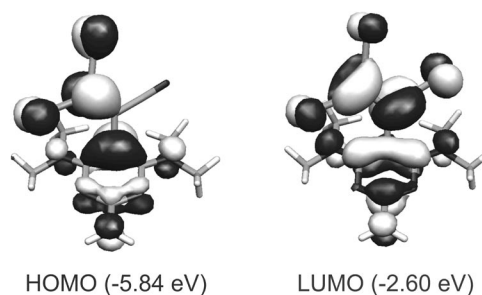


Figure 4. Electron density contours (0.03 eBohr⁻³) and energies (within parentheses) calculated for the HOMO and LUMO of **7a**.

To investigate the nature of the electronic transitions that give rise to the absorption bands observed experimentally in the UV/Vis spectra, the electronically excited states of compounds **2a**, **4a** and **7a** were calculated by using the time-

dependent DFT (TDDFT) approach, the B3LYP/6-31G** optimized geometries and the polarized continuum model (PCM) to take the interaction with the solvent into account. Calculations predict that the lowest-energy absorption bands – observed at 299 nm for **2a**, 411 nm for **4a**, and 454 nm for **7a** – are associated with electronic transitions that imply, in all three cases, the HOMO→LUMO one-electron excitation. The corresponding electronic transitions are calculated in CH₃CN at 4.49 eV (276 nm) for **2a**, 3.39 eV (365 nm) for **4a**, and 2.98 eV (417 nm) for **7a** and have oscillator strengths (*f*) of 0.17, 0.44 and 0.39. The theoretical results slightly underestimate the energies of the absorption bands but correctly reproduce the bathochromic shifts observed on passing from compounds **2** to **4** and from **4** to **7**, due to the narrowing of the HOMO–LUMO gap along this series.

The absorptions above 400 nm displayed by the push-pull compounds **4** and **7** are therefore assigned to π – π^* HOMO→LUMO one-electron promotions. As discussed above, these orbitals are spread over the whole molecule, and the transition implies no significant electron-density transfer from the dialkylamino groups to the electron-acceptor group (see Figure 4). This is corroborated by the values of the dipole moments, which remain almost unaffected on passing from the ground state (**4a**: 9.2 D, **7a**: 10.3 D) to the first excited state (**4a**: 9.3 D, **7a**: 9.9 D) involved in the electronic transition. The absorption bands cannot therefore be classified as intramolecular charge-transfer bands as initially expected. This is experimentally supported by the small solvatochromism observed for **4a**. The absorption maximum measured in CHCl₃ (407 nm), which has a low dielectric constant ($\epsilon = 4.9$), is very similar to that recorded in CH₃CN (411 nm), which is a much more polar solvent ($\epsilon = 36.6$).

Redox Properties

The electrochemical properties of compounds **2a–d**, **3**, **4a–d**, **7a–d** and of the reference compound **8** (Scheme 1) were studied at room temperature by cyclic voltammetry (CV) of acetonitrile solutions containing tetrabutylammonium hexafluorophosphate (TBAPF₆, 0.1 M). Oxidation and reduction potentials (Table 2) were measured with an Ag/AgNO₃ reference electrode, a glassy carbon working electrode and a platinum counter electrode.

Compound **8**, bearing only electron-donating dialkylamino groups, shows an oxidation wave at +0.871 V. The oxidation wave shifts to slightly higher anodic potentials for compounds **2a–d** (from +0.930 to +1.060 V) and **4a–d** (from +0.894 to +1.060 V), most probably due to the presence of the electron-withdrawing formyl and dicyanovinyl groups within the same structure. Theoretical calculations predict similar energies for the HOMOs of **2a** (–5.54 eV) and **4a** (–5.57 eV) which, in a first approach, accounts for the similar oxidation potentials measured for **2a–d** and **4a–d**. In compound **7a** the obtained HOMO is more stable (–5.84 eV) and the oxidation potentials of compounds **7a–d** are shifted to higher values (from +1.107 to +1.190 V).

As displayed in Figure 5, no reduction waves for compounds **2a–d** are observed under these experimental conditions, due to the very weak electron-acceptor character of the formyl group attached to the pyrimidine ring. In contrast, compound **3**, bearing no dialkylamino units, shows no oxidation process and instead exhibits two reduction waves at –1.289 and –1.842 V, due to the presence of chlorine atoms and of the dicyanovinyl group. Compounds **4a–d** again incorporate dialkylamino groups and each show a single reduction wave around –1.95 V that can reasonably be assigned to the reduction of the dicyanovinyl unit. In contrast, compounds **7a–d**, bearing the stronger electron-acceptor tricyanovinyl group, each present a first reduction wave around –1.10 V and a second reduction process between –1.854 and –2.119 V.

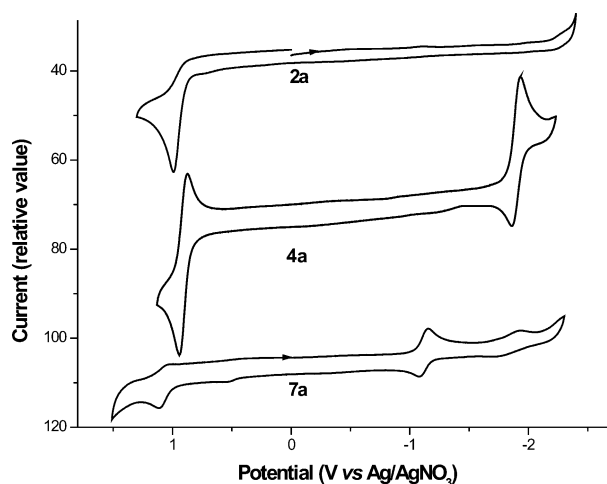


Figure 5. Cyclic voltammograms for compounds **2a**, **4a** and **7a** in CH₃CN containing TBAPF₆ (0.1 M) as supporting electrolyte.

The oxidized (cation) and reduced (anion and dianion) species of **7a** were calculated at the B3LYP/6-31G** level to provide a deeper understanding of the oxidation/reduction processes. As summarized in Table 1, oxidation and reduction processes affect all the geometrical parameters of the molecule, because both the HOMO (that is, the orbital from which electrons are removed) and the LUMO (that is, the orbital to which extra electrons are attached) are spread over the whole molecule (see Figure 4). The cation preserves the conformation of the neutral molecule and the electron is extracted from all the groups constituting the molecule. For instance, the charge on the tricyanovinyl unit changes from –0.44 e in the neutral molecule to –0.05 e in the cation and the sum of the charges of the dialkylamino groups increases from +0.20 e to +0.47 e.

Upon reduction to the radical anion, the tricyanovinyl group twists around the C(5)–C(8) bond (1.496 Å), and the **7a**^{•–} species presents a perpendicular structure similar to that depicted in Figure 2 (c) as the most stable conformation. The extra electron preferentially resides on the tricyanovinyl group, which now has a charge of –1.00 e, but also affects the rest of the molecule. The dianion behaves in a

different way. The most stable structure depicted in Figure 6 (a) resembles that of the neutral molecule (Figure 2, a), but now the C(CN)₂ group is twisted around the C(8)–C(9) bond, which has lengthened to 1.509 Å, to avoid the steric contacts. In **7a**²⁻, the tricyanovinyl unit accumulates a total charge of –1.56 e and the dialkylamino units have small negative charges of –0.11 e and are more pyramidalized, due to the electron density they have recuperated. Species **7a**²⁻ presents a second conformation (Figure 6, b) in which the tricyanovinyl group is perpendicular to the ring and the C(CN)₂ group is also rotated around the C(8)–C(9) bond. This conformation is less stable by only 1.46 kcal mol⁻¹ (0.63 kcal mol⁻¹ in CH₃CN) and allows a higher concentration of the charge on the tricyanovinyl unit (–1.82 e). This conformation would be easily attained in the second reduction process because the radical **7a**^{•-} species already presents a perpendicular conformation.

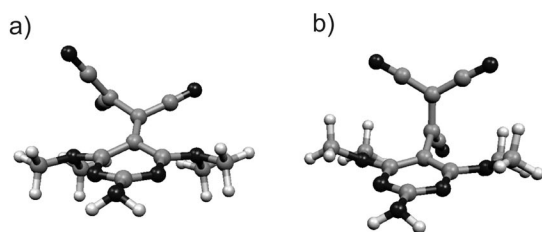


Figure 6. Minimum-energy conformations calculated for **7a**²⁻ at the B3LYP/6-31G** level.

Conclusions

In summary, we have carried out the synthesis of a series of aminopyrimidine-based donor–acceptor systems **4a–d**, **7a–d** – each bearing two electron-donor dialkylamino groups and either a dicyanovinyl (**4a–d**) or a tricyanovinyl (**7a–d**) group as an electron-acceptor unit – from commercially available 2-amino-4,6-dihydropyrimidine (ADHP). The presence of donor and acceptor groups in conjugation through the pyrimidine ring gives rise to rather complex electronic and geometrical structures, in which the push–pull effect and the aromatic behaviour of the pyrimidine ring are in competition. Interestingly, the experimental observations (FTIR, UV/Vis, CV, X-ray diffraction) and theoretical calculations (DFT) carried out at the B3LYP/6-31G** level reveal that the electronic properties of these systems are strongly influenced by the steric interactions between the dicyanovinyl (**4a–d**) or tricyanovinyl (**7a–d**) groups and the adjacent dialkylamino units. The geometries adopted by the molecules are distorted from planarity and favour charge transfer from the donor groups to the electron-withdrawing tricyanovinyl or dicyanovinyl group. The low-energy absorption band shown in the visible is not due to the expected intramolecular charge transfer band typically observed for push–pull chromophores, but it is attributed to a π – π^* electronic transition that involves the whole molecule and is poorly affected by solvent polarity.

The above findings reveal the subtle trade-off existing between aromaticity, push–pull interactions and steric effects when defining the electronic properties of complex chromophores such as those examined in this study.

Experimental Section

General: Commercially available starting materials, reagents and solvents were used as supplied. TLC analyses were performed on Merck TLC plates (aluminium sheets, silica gel 60 F₂₅₄). Mass spectra (EI) were run with a Shimadzu QP-2010 instrument. ¹H NMR and ¹³C NMR spectra were measured in a Bruker AMX 400 at 25 °C, unless otherwise indicated. Infrared spectra were recorded as KBr pellets with a Shimadzu FT-IR 8400 spectrometer. UV/Vis spectra were recorded in a Varian Cary 50 spectrometer in CH₃CN as solvent. Melting points were recorded with a Sanyo Gallenkamp digital melting-point apparatus.

Electrochemical measurements were performed on an Autolab PGStat 30 apparatus with a three-electrode configuration system. The measurements were carried out in CH₃CN solutions containing tetrabutylammonium hexafluorophosphate (TBAPF₆, 0.1 M). A glassy carbon electrode (3 mm diameter) was used as the working electrode, and a platinum wire and an Ag/AgNO₃ electrode were employed as the counter and the reference electrodes, respectively. Both the counter and the reference electrodes were directly immersed in the electrolyte solution. The surface of the working electrode was polished with commercial alumina prior to use. Solutions were deaerated by bubbling argon for a few minutes prior to each voltammetric measurement. Unless otherwise specified the scan rate was 100 mV s⁻¹.

X-ray Analysis: Suitable crystals for X-ray diffraction were obtained by crystallization from CH₂Cl₂/CH₃OH. Data collection for **7a** was carried out at room temperature on a Bruker Smart CCD diffractometer with use of graphite-monochromated Mo-K α radiation (λ = 0.71073 Å) operating at 50 kW and 30 mA. The data were collected over a hemisphere of the reciprocal space by combination of three exposure sets. Each exposure of 10 s covered 0.3 in ω . The cell parameters were determined and refined by a least-squares fit of all reflections. The first 100 frames were recollected at the end of the data collection to monitor crystal decay, and no appreciable decay was observed. The structure was solved by direct methods and refined by full-matrix, least-squares procedures on F^2 (SHELXL-97).^[17] All non-hydrogen atoms were refined anisotropically. The hydrogen atoms were included in their calculated positions and refined riding on the respective carbon atoms with a common isotropic thermal parameter, with the exception of H6A and H6B bonded to N6, which were located on a difference Fourier map and included in the final refinement.

CCDC-645204 contains the supplementary crystallographic data for compound **7a**. These data can be obtained free of charge via www.ccdc.cam.ac.uk/conts/retrieving.html (or from the Cambridge Crystallographic Data Centre, 12 Union Road, Cambridge CB2 1EZ, UK; fax: (+44)-1223-336033; or deposit@ccdc.cam.ac.uk).

Computational Details: All theoretical calculations were carried out by the DFT approach using the C.02 revision of the Gaussian 03 program package.^[21] DFT calculations were performed using Becke's three-parameter B3LYP exchange-correlation functional^[22] and the 6-31G** and 6-311+G** basis sets.^[23] Radical cations and anions were treated as open-shell systems and were computed using spin-unrestricted UB3LYP wavefunctions. Vertical electronic excitations energies were determined by the TDDFT approach.^[24] Nu-

merous previously reported applications indicate that TDDFT employing current exchange-correlation functionals performs significantly better than HF-based single-excitation theories for the low-lying valence excited states. Net atomic charges were calculated by the NPA analysis^[25] included in the natural bond orbital (NBO) algorithm proposed by Weinhold and co-workers.^[26] Solvent effects were considered within the SCRf (self-consistent-reaction-field) theory with use of the polarized continuum model (PCM) approach to model the interaction with the solvent.^[27] The PCM model regards the solvent as a continuous medium with a dielectric constant ϵ and represents the solute by means of a cavity built with a number of interlaced spheres.^[28]

2-Amino-4,6-dichloro-5-formylpyrimidine (1): Dry dimethylformamide (35 mL) was added dropwise to a previously cooled solution (0 °C) of pristine phosphorus oxychloride (108 mL, 1.18 mol), and the resulting mixture was stirred for 15 min. The reaction mixture was warmed gently to produce a clear solution, and then 2-amino-6-hydroxy-4-(3*H*)-pyrimidinone (28 g, 0.22 mol) was added in small portions with stirring over a period of 30 min. Heating the mixture on a steam bath for 5 h gave a dark red–brown solution. Excess phosphorus oxychloride (about 15 mL) was removed by distillation in vacuo, leaving a dark red–brown viscous oil. The oil was mixed with crushed ice (1500 mL) and allowed to stand at room temperature overnight; the resulting mixture consisted of a red-orange solution and a yellow-brown solid. The solid was collected by filtration. The filtrate was treated with concentrated ammonium hydroxide in portions to pH = 7.0. The precipitated yellow–brown solid was collected by filtration. The combined precipitates were vacuum-dried at room temperature overnight and then extracted with hot ethyl acetate (6 × 400 mL), leaving a brown insoluble residue that was discarded. Upon cooling, a yellow precipitate formed in the combined ethyl acetate extracts, and filtration gave **1** (21.88 g, 51%), m.p. > 130 °C (dec.). ¹H NMR ([D₆]DMSO, 400 MHz): δ = 8.47 (s, 2 H), 10.05 (s, 1 H) ppm. ¹³C NMR ([D₆]DMSO, 100 MHz): δ = 112.8, 161.6, 163.1, 184.6 ppm. FTIR (KBr): $\tilde{\nu}$ = 3424, 3322, 1671, 1641 cm⁻¹. MS (EI): m/z = 195 [M]⁺, 193, 191, 190.

General Procedure for the Synthesis of Compounds 2a–d: The appropriate secondary amine (1 mL) was added dropwise to a stirring solution of 2-amino-4,6-dichloro-5-formylpyrimidine (**1**, 100 mg, 0.52 mmol) in ethanol (3 mL), and the system was heated to reflux for 20 min. The solution was evaporated to dryness and the residue was recrystallized from ethyl acetate to afford **2a–c**. Compound **2d** was purified by flash chromatography (silica gel, CH₂Cl₂/MeOH, 20:1).

2-Amino-4,6-bis(dimethylamino)-5-formylpyrimidine (2a): 102.16 mg, 94%, m.p. 191–193 °C. ¹H NMR ([D₆]DMSO, 400 MHz): δ = 3.06 (s, 12 H), 6.55 (s, 2 H), 9.04 (s, 1 H) ppm. ¹³C NMR ([D₆]DMSO, 100 MHz): δ = 39.9, 91.1, 162.0, 166.9, 178.0 ppm. FTIR (KBr): $\tilde{\nu}$ = 3337, 3202, 2922, 1630, 1542 cm⁻¹. UV/Vis (CH₃CN): λ_{\max} (ϵ) [nm]: 299.0 (1.04 × 10⁴). MS (EI): m/z = 209 [M]⁺, 42.

2-Amino-4,6-bis(diethylamino)-5-formylpyrimidine (2b): 110.24 mg, 80%, m.p. 114–116 °C. ¹H NMR ([D₆]DMSO, 400 MHz): δ = 1.20 (t, J = 7.2 Hz, 12 H), 3.60 (q, J = 7.0 Hz, 8 H), 4.83 (s, 2 H), 9.09 (s, 1 H) ppm. ¹³C NMR ([D₆]DMSO, 100 MHz): δ = 13.4, 44.1, 93.6, 162.3, 167.6, 179.1 ppm. FTIR (KBr): $\tilde{\nu}$ = 3375, 3161, 2974, 2753, 1662, 1618 cm⁻¹. UV/Vis (CH₃CN): λ_{\max} (ϵ) [nm]: 302.0 (1.21 × 10⁴). MS (EI): m/z = 265 [M]⁺, 72.

2-Amino-4,6-bis(benzylmethylamino)-5-formylpyrimidine (2c): 150.18 mg, 80%, m.p. 214–215 °C. ¹H NMR ([D₆]DMSO, 400 MHz): δ = 3.09 (s, 6 H), 4.86 (s, 4 H), 5.01 (brs, 2 H), 7.24–7.34 (m, 10 H), 9.31 (s, 1 H) ppm. ¹³C NMR ([D₆]DMSO, 100 MHz):

δ = 39.51, 55.12, 92.49, 127.3, 127.7, 128.5, 137.0, 162.4, 168.1, 179.0 ppm. FTIR (KBr): $\tilde{\nu}$ = 3481, 3298, 3027, 2918, 2795, 1609 cm⁻¹. UV/Vis (CH₃CN): λ_{\max} (ϵ) [nm]: 303.0 (1.32 × 10⁴). MS (EI): m/z = 361 [M]⁺, 91.

2-Amino-4,6-bis(dibenzylamino)-5-formylpyrimidine (2d): 246.65 mg, 98%, m.p. 151–156 °C. ¹H NMR ([D₆]DMSO, 400 MHz): δ = 4.63 (s, 8 H), 5.02 (s, 2 H), 7.09–7.38 (m, 20 H), 9.36 (s, 1 H) ppm. ¹³C NMR ([D₆]DMSO, 100 MHz): δ = 53.1, 94.1, 127.2–128.6, 162.5, 168.4, 179.7 ppm. FTIR (KBr): $\tilde{\nu}$ = 3445, 3292, 3026, 2926, 2763, 1602, 1500 cm⁻¹. UV/Vis (CH₃CN): λ_{\max} (ϵ) [nm]: 299.1 (1.19 × 10⁴). MS (EI): m/z = 484 [M]⁺, 91.

2-Amino-4,6-dichloro-5-(2,2-dicyanovinyl)pyrimidine (3): 2-Amino-4,6-dichloro-5-formylpyrimidine (**1**, 384 mg, 2 mmol) and malononitrile (141 mg, 2 mmol) were dissolved in ethanol (3 mL), and calcium chloride (10 mg) and triethylamine (20 mg) were added. The solution was stirred for 30 min at room temperature, water (8 mL) was then added, and the system was stirred for 30 additional minutes. A yellowish solid was formed, filtered off and recrystallized from ethanol (358.50 mg, 75%); m.p. 198 °C (decomp.). ¹H NMR ([D₆]DMSO, 400 MHz): δ = 8.47 (s, 2 H), 10.08 (s, 1 H) ppm. ¹³C NMR ([D₆]DMSO, 100 MHz): δ = 89.1, 112.8, 159.7, 163.1, 184.6 ppm. FTIR (KBr): $\tilde{\nu}$ = 3325, 3194, 2231, 1654, 1558 cm⁻¹. UV/Vis (CH₃CN): λ_{\max} (ϵ) [nm]: 335.0 (1.23 × 10⁴). MS (EI): m/z = 239 [M]⁺, 241, 190.

General Procedure for the Synthesis of Compounds 4a–d: The appropriate secondary amine (1 mL) was added dropwise to a solution of 2-amino-4,6-dichloro-5-(2,2-dicyanovinyl)pyrimidine (**3**, 150 mg, 0.63 mmol) in absolute ethanol (10 mL), and the solution was stirred and heated to reflux for 40 min. The solution was then cooled to room temperature. In all cases a yellowish solid precipitated, except in the case of **4b**, in which an orangish solid was obtained. The corresponding solids were filtered off and recrystallized from ethanol.

2-Amino-5-(2,2-dicyanovinyl)-4,6-bis(dimethylamino)pyrimidine (4a): 131.15 mg, 81%, m.p. 268–270 °C. ¹H NMR ([D₆]DMSO, 400 MHz): δ = 3.09 (s, 12 H), 7.09 (s, 1 H), 7.23 (s, 2 H) ppm. ¹³C NMR ([D₆]DMSO, 100 MHz): δ = 51.3, 91.0, 116.8, 120.1, 147.3, 162.6, 166.0 ppm. FTIR (KBr): $\tilde{\nu}$ = 3381, 3201, 2192, 1653 cm⁻¹. UV/Vis (CH₃CN): λ_{\max} (ϵ) [nm]: 270.1 (2.78 × 10⁴), 332.0 (2.12 × 10⁴), 411.0 (4.46 × 10⁴). MS (EI): m/z = 257 [M]⁺, 192, 44.

2-Amino-5-(2,2-dicyanovinyl)-4,6-bis(diethylamino)pyrimidine (4b): 153.81 mg, 78%, m.p. 200–201 °C. ¹H NMR ([D₆]DMSO, 400 MHz): δ = 1.17 (t, J = 7.0 Hz, 12 H), 3.54 (q, J = 7.0 Hz, 8 H), 6.83 (s, 1 H), 7.31 (s, 2 H) ppm. ¹³C NMR ([D₆]DMSO, 100 MHz): δ = 13.48, 43.8, 92.5, 116.8, 120.4, 145.2, 162.8, 166.3 ppm. FTIR (KBr): $\tilde{\nu}$ = 3388, 3207, 2933, 2200, 1650, 1577 cm⁻¹. UV/Vis (CH₃CN): λ_{\max} (ϵ) [nm]: 270.0 (0.64 × 10⁴), 336.0, 417.0 (1.69 × 10⁴). MS (EI): m/z = 313 [M]⁺, 69.

2-Amino-4,6-bis(benzylmethylamino)-5-(2,2-dicyanovinyl)pyrimidine (4c): 239.63 mg, 93%, m.p. 211–212 °C. ¹H NMR ([D₆]DMSO, 400 MHz): δ = 2.98 (s, 6 H), 4.79 (brs, 4 H), 7.19 (s, 1 H), 7.23–7.36 (m, 10 H), 7.42 (s, 2 H) ppm. ¹³C NMR ([D₆]DMSO, 100 MHz): δ = 37.2, 52.8, 90.9, 116.7, 119.7, 127.3, 127.6, 128.5, 147.4, 136.6, 162.9 ppm. FTIR (KBr): $\tilde{\nu}$ = 3488, 3375, 2201, 1622 cm⁻¹. UV/Vis (CH₃CN): λ_{\max} (ϵ) [nm]: 271.9 (1.64 × 10⁴), 333.9, 413.0 (3.89 × 10⁴). MS (EI): m/z = 409 [M]⁺, 394, 344, 91.

2-Amino-4,6-bis(dibenzylamino)-5-(2,2-dicyanovinyl)pyrimidine (4d): 335.16 mg, 95%, m.p. 205–208 °C. ¹H NMR ([D₆]DMSO, 400 MHz): δ = 4.44 (brs, 8 H), 6.74 (s, 1 H), 7.02–7.36 (m, 20 H), 7.63 (s, 2 H) ppm. ¹³C NMR ([D₆]DMSO, 100 MHz): δ = 52.2, 93.0, 116.4, 118.7, 126.7–128.5, 136.3, 145.6, 162.7, 166.2 ppm.

FTIR (KBr): $\tilde{\nu}$ = 3474, 3326, 2204, 1627, 1568 cm^{-1} . UV/Vis (CH_3CN): λ_{max} (ϵ) [nm]: 282.0 (6.10×10^4), 340.0 (5.87×10^4), 417.0 (7.31×10^4). MS (EI): m/z = 560 $[\text{M}]^+$, 470.

2-Amino-4,6-dichloro-5-(1,2,2-tricyanoethyl)pyrimidine (5): 2-Amino-4,6-dichloro-5-(2,2-dicyanovinyl)pyrimidine (**3**, 150 mg, 0.63 mmol) was suspended in ethanol (2 mL), KCN (42 mg, 0.65 mmol) in water (0.1 mL) was then added dropwise, and the mixture was stirred at room temperature for 30 min. HCl (0.5 M, 2.4 mL) was added, and the solution was stirred overnight. A yellowish solid was formed, filtered off, washed with hexane and recrystallized from ethanol. (137.42 mg, 82%), m.p. 242–244 °C decomp. ^1H NMR ($[\text{D}_6]\text{DMSO}$, 400 MHz): δ = 5.72 (d, J = 10.1 Hz, 1 H), 5.94 (d, J = 10.1 Hz, 1 H), 8.07 (s, 2 H) ppm. ^{13}C NMR ($[\text{D}_6]\text{DMSO}$, 100 MHz): δ = 25.7, 31.6, 105.8, 110.9, 111.1, 114.2, 161.2 ppm. FTIR (KBr): $\tilde{\nu}$ = 3440, 3326, 2917, 2258, 1658, 1580 cm^{-1} . MS (EI): m/z = 266 $[\text{M}]^+$, 201.

2-Amino-4,6-dichloro-5-(tricyanovinyl)pyrimidine (6): 2-Amino-4,6-dichloro-5-(1,2,2-tricyanoethyl)pyrimidine (**5**, 30 mg, 0.11 mmol), NBS (78.3 mg, 0.44 mmol) and AIBN (5 mg) were dissolved in acetonitrile (3 mL) and stirred at room temperature for 30 min. The organic solvent was evaporated in vacuo to yield a yellowish solid, which was washed with hexane and recrystallized from ethyl acetate (26.53 mg, 91%), m.p. 101–104 °C. ^1H NMR ($[\text{D}_6]\text{DMSO}$, 400 MHz): δ = 7.30 (s, 2 H) ppm. ^{13}C NMR ($[\text{D}_6]\text{DMSO}$, 100 MHz): δ = 101.8, 108.5, 109.0, 106.3, 111.1, 158.7, 161.7–161.8 ppm. FTIR (KBr): $\tilde{\nu}$ = 3353, 3206, 2199, 1711, 1582 cm^{-1} . MS (EI): m/z = 265 $[\text{M}]^+$, 264, 229.

General Procedure for the Synthesis of Compounds 7a–d: The appropriate secondary amine (1.0 mL) was added dropwise to a solution of 2-amino-4,6-dichloro-5-(tricyanovinyl)pyrimidine (**6**, 100 mg, 0.38 mmol) in absolute ethanol (10 mL). The solution was then stirred and heated to reflux for 20 min. The organic solvent was evaporated in vacuo, and the residue was purified by flash chromatography (silica gel, $\text{CH}_2\text{Cl}_2/\text{MeOH}$, 20:1).

2-Amino-4,6-bis(dimethylamino)-5-(tricyanovinyl)pyrimidine (7a): 72.87 mg, 68%, m.p. 190–195 °C (dec.). ^1H NMR ($[\text{D}_6]\text{DMSO}$, 400 MHz): δ = 5.47 (s, 2 H), 3.25 (s, 12 H) ppm. ^{13}C NMR ($[\text{D}_6]\text{DMSO}$, 100 MHz): δ = 34.1, 98.5, 114.7, 162.1, 164.6 ppm. FTIR (KBr): $\tilde{\nu}$ = 3419, 3330, 3210, 2925, 2196, 2177, 1595 cm^{-1} . UV/Vis (CH_3CN): λ_{max} (ϵ) [nm]: 281.9 (15.0×10^4), 454.0 (13.9×10^4). MS (EI): m/z = 282 $[\text{M}]^+$, 242, 71.

2-Amino-4,6-bis(diethylamino)-5-(tricyanovinyl)pyrimidine (7b): 82.73 mg, 70%, m.p. 210–211 °C dec. ^1H NMR ($[\text{D}_6]\text{DMSO}$, 400 MHz): δ = 8.48 (s, 2 H), 4.32 (q, J = 9.4 Hz, 8 H), 1.34 (t, J = 9.4 Hz, 12 H) ppm. ^{13}C NMR ($[\text{D}_6]\text{DMSO}$, 100 MHz): δ = 35.2, 49.7, 99.6, 115.9, 120.0, 123.2, 163.2, 165.7 ppm. FTIR (KBr): $\tilde{\nu}$ = 3418, 3328, 3195, 2922, 2203, 2199, 2185, 1580 cm^{-1} . UV/Vis (CH_3CN): λ_{max} (ϵ) [nm]: 274.0 (19.9×10^4), 459.9 (1.69×10^4). MS (EI): m/z = 311 $[\text{M}]^+$, 296, 190.

2-Amino-4,6-bis(methylbenzylamino)-5-(tricyanovinyl)pyrimidine (7c): 94 mg, 57%, m.p. 200–203 °C dec. ^1H NMR ($[\text{D}_6]\text{DMSO}$, 400 MHz): δ = 8.17 (s, 2 H), 7.31 (m, 10 H), 4.85 (s, 4 H), 2.47 (s, 6 H) ppm. ^{13}C NMR ($[\text{D}_6]\text{DMSO}$, 100 MHz): δ = 55.9, 94.2, 130.5, 130.8, 131.7, 139.8, 169.9 ppm. FTIR (KBr): $\tilde{\nu}$ = 3421, 3324, 2930, 2922, 2199, 2186, 1576 cm^{-1} . UV/Vis (CH_3CN): λ_{max} (ϵ) [nm]: 273.9 (17.8×10^4), 460.0 (7.24×10^4). MS (EI): m/z = 434 $[\text{M}]^+$, 419, 91.

2-Amino-4,6-bis(dibenzylamino)-5-(tricyanovinyl)pyrimidine (7d): 155.88 mg, 70%, m.p. 181–184 °C dec. ^1H NMR ($[\text{D}_6]\text{DMSO}$, 400 MHz): δ = 1.55 (s, 8 H), 4.53 (s, 2 H), 6.93 (m, 20 H) ppm. ^{13}C NMR ($[\text{D}_6]\text{DMSO}$, 100 MHz): δ = 46.6, 99.4, 128.3, 129.4, 129.6, 146.5, 158.2, 160.5, 163.8, 167.1 ppm. FTIR (KBr): $\tilde{\nu}$ = 3420, 3318,

2952, 2213, 2200, 1581 cm^{-1} . MS (EI): m/z = 586 $[\text{M}]^+$, 521, 495, 334, 91. UV/Vis (CH_3CN): λ_{max} (ϵ) [nm]: 274.0 (72.3×10^4), 465.0 (27.3×10^4).

2-Amino-4,6-bis(diethylamino)-5H-pyrimidine (8): 2-Amino-4,6-dichloropyrimidine (200 mg, 1.23 mmol) was dissolved in absolute ethanol (10 mL). Diethylamine (1.0 mL) was added dropwise, the solution was stirred and heated to reflux for 40 min, the solvent was evaporated in vacuo, and the residues were purified by flash chromatography (silica gel, CH_2Cl_2) (244.87 mg, 84%), m.p. 191 °C. ^1H NMR ($[\text{D}_6]\text{DMSO}$, 400 MHz): δ = 1.18 (t, J = 7.6 Hz, 12 H), 2.87 (q, J = 7.6 Hz, 8 H), 8.80 (brs, 3 H) ppm. ^{13}C NMR ($[\text{D}_6]\text{DMSO}$, 100 MHz): δ = 12.7, 89.8, 158.7, 162.0, 162.5 ppm. FTIR (KBr): $\tilde{\nu}$ = 3309, 3164, 2975, 1639, 1572 cm^{-1} . UV/Vis (CH_3CN): λ_{max} (ϵ) [nm]: 289.0 (1.60×10^4). MS (EI): m/z = 237 $[\text{M}]^+$, 200, 185, 171, 157, 67.

Acknowledgments

This work has been supported by COLCIENCIAS (Colombia), the Universidad del Valle (Colombia), the Spanish Ministerio de Educación y Ciencia (MEC) (grants CTQ2005-02609/BQU and CTQ2006-14987-C02-02/BQU), by the Comunidad de Madrid (P-PPQ-000225-0505), by the Generalitat Valenciana, and by funds of the Fondo Europeo de Desarrollo Regional (FEDER) (CTQ2006-14987-C02-02/BQU). M. A. H. would like to thank the MEC for a “Ramón y Cajal” contract.

- [1] a) Special issue dedicated to aromaticity, see: P. v. R. Schleyer, *Chem. Rev.* **2001**, *101*, 1115–1566; b) Special issue dedicated to aromaticity, see: P. v. R. Schleyer, *Chem. Rev.* **2005**, *105*, 3433–3947.
- [2] a) R. Herges, *Chem. Rev.* **2006**, *106*, 4820–4842; b) D. Ajami, O. Oeckler, A. Simon, R. Herges, *Nature* **2003**, *426*, 819–821; c) see also: International Symposium on Novel Aromatic Compounds (ISNA-12), Awaji-Island, Japan, July 2007.
- [3] a) G. M. Blackburn, M. J. Gait, *Nucleic Acids in Chemistry and Biology*, Oxford University Press, Oxford, **1996**; b) J. S. Kwiatkowski, B. Pulmann, *Adv. Heterocycl. Chem.* **1975**, *18*, 199–335; c) A. Alparone, A. Millefiori, S. Millefiori, *Chem. Phys.* **2005**, *312*, 261–274.
- [4] A. El-Ghayoury, A. P. H. J. Schenning, P. A. Van Hal, J. K. J. Van Duren, R. A. J. Janssen, E. W. Meijer, *Angew. Chem.* **2001**, *113*, 3772–3775; *Angew. Chem. Int. Ed.* **2001**, *40*, 3660–3663.
- [5] Y. J. Kim, J. H. Kim, M.-S. Kang, M. J. Lee, J. Won, J. Ch. Lee, Y. S. Kang, *Adv. Mater.* **2004**, *16*, 1753–1757.
- [6] Ch.-H. Huang, N. D. McClenaghan, A. Kuhn, G. Bravic, D. M. Bassani, *Tetrahedron* **2006**, *62*, 2050–2059.
- [7] T. Hegmann, J. Kain, S. Diele, B. Schubert, H. Bögel, C. Tschierske, *J. Mater. Chem.* **2003**, *13*, 991–1003.
- [8] For a review, see: T. Verbiest, S. Houbrechts, M. Kauranen, K. Clays, A. Persoons, *J. Mater. Chem.* **1997**, *7*, 2175–2189.
- [9] E. Botek, F. Castet, B. Champagne, *Chem. Eur. J.* **2006**, *12*, 8687–8695.
- [10] E. M. Priego, L. Sánchez, M. A. Herranz, N. Martín, R. Viruela, E. Ortí, *Org. Biomol. Chem.* **2007**, *5*, 1201–1209.
- [11] T. J. Thomas, R. Otteman, *Heterocycles* **1983**, *20*, 1805–1809.
- [12] J. S. Chappell, A. N. Bloch, W. A. Bryden, M. Maxfield, T. O. Poehler, D. O. Cowan, *J. Am. Chem. Soc.* **1981**, *103*, 2442–2443.
- [13] P. De la Cruz, N. Martín, F. Miguel, C. Seoane, A. Albert, F. H. Cano, A. Gonzalez, J. M. Pingarrón, *J. Org. Chem.* **1992**, *57*, 6192–6198.
- [14] N. Martín, J. L. Segura, C. Seoane, P. de la Cruz, F. Langa, E. Ortí, R. Viruela, P. M. Viruela, *J. Org. Chem.* **1995**, *60*, 4077–4084.

- [15] E. Ortí, R. Viruela, P. M. Viruela, *J. Phys. Chem.* **1996**, *100*, 6138–6146.
- [16] a) N. Martín, M. Hanack, *J. Chem. Soc. Chem. Commun.* **1988**, 1522–1524; b) N. Martín, R. Behnisch, M. Hanack, *J. Org. Chem.* **1989**, *54*, 2563–2568.
- [17] G. M. Sheldrick, *SHELX97, Program for Refinement of Crystal Structure*, University of Göttingen, Göttingen, Germany, **1997**.
- [18] L. Fernholt, C. Romming, *Acta Chem. Scand. Ser. A* **1978**, *32*, 271–273.
- [19] Harmonic frequency calculations on the optimized geometries confirmed the four structures as minima of the potential energy hypersurface, as no imaginary frequency was obtained.
- [20] T. Michinobu, C. Boudon, J.-P. Gisselbrecht, P. Seiler, B. Frank, N. N. P. Moonen, M. Gross, F. Diederich, *Chem. Eur. J.* **2006**, *12*, 1889–1905.
- [21] M. J. Frisch, G. W. Trucks, H. B. Schlegel, G. E. Scuseria, M. A. Robb, J. R. Cheeseman Jr, J. A. Montgomery, T. Vreven, K. N. Kudin, J. C. Burant, J. M. Millam, S. S. Iyengar, J. Tomasi, V. Barone, B. Mennucci, M. Cossi, G. Scalmani, G. Rega, G. A. Petersson, H. Nakatsuji, M. Hada, M. Ehara, K. Toyota, R. Fukuda, J. Hasegawa, M. Ishida, T. Nakajima, Y. Honda, O. Kitao, H. Nakai, M. Klene, X. Li, J. E. Knox, H. P. Hratchian, J. B. Cross, V. Bakken, C. Adamo, J. Jaramillo, R. Gomperts, R. E. Stratmann, O. Yazyev, A. J. Austin, R. Cammi, C. Pomelli, J. W. Ochterski, P. Y. Ayala, K. Morokuma, G. A. Voth, P. Salvador, J. J. Dannenberg, V. G. Zakrzewski, S. Dapprich, A. D. Daniels, M. C. Strain, O. Farkas, D. K. Malick, A. D. Rabuck, K. Raghavachari, J. B. Foresman, J. V. Ortiz, Q. Cui, A. G. Baboul, S. Clifford, J. Cioslowski, B. B. Stefanov, G. Liu, A. Liashenko, P. Piskorz, I. Komaromi, R. L. Martin, D. J. Fox, T. Keith, M. A. Al-Laham, C. Y. Peng, A. Nanayakkara, M. Challacombe, P. M. W. Gill, B. Johnson, W. Chen, M. W. Wong, C. Gonzalez, J. A. Pople, *Gaussian 03, Revision C.02*, Gaussian, Inc., Wallingford CT, **2004**.
- [22] A. D. Becke, *J. Chem. Phys.* **1993**, *98*, 1372–1377.
- [23] a) M. M. Francl, W. J. Pietro, W. J. Hehre, J. S. Binkley, M. S. Gordon, D. J. Defrees, J. A. Pople, *J. Chem. Phys.* **1982**, *77*, 3654–3665; b) W. J. Hehre, L. Radom, P. v. R. Schelyer, J. A. Pople, *Ab initio Molecular Orbital Theory*, Wiley, New York, **1986**.
- [24] a) E. Runge, E. K. U. Gross, *Phys. Rev. Lett.* **1984**, *52*, 997–1000; b) E. K. U. Gross, W. Kohn, *Adv. Quantum Chem.* **1990**, *21*, 255–291; c) E. K. U. Gross, C. A. Ullrich, U. J. Gossmann, *Density Functional Theory* (Eds.: E. K. U. Gross, R. M. Dreizler), Plenum Press, New York, **1995**, p. 149; d) M. E. Casida, *Recent Advances in Density Functional Methods, Part I* (Ed.: D. P. Chong), World Scientific, Singapore, **1995**, p. 155.
- [25] a) A. E. Reed, F. Weinhold, *J. Chem. Phys.* **1983**, *78*, 4066–4073; b) A. E. Reed, R. B. Weinstock, F. Weinhold, *J. Chem. Phys.* **1985**, *83*, 735–746.
- [26] A. E. Reed, L. A. Curtiss, F. Weinhold, *Chem. Rev.* **1988**, *88*, 899–926.
- [27] a) J. Tomasi, M. Persico, *Chem. Rev.* **1994**, *94*, 2027–2094; b) C. S. Cramer, D. G. Truhlar, *Solvent Effects and Chemical Reactivity* (Eds.: O. Tapia, J. Bertrán), Kluwer, Dordrecht, **1996**, p. 1.
- [28] a) S. Miertus, E. Scrocco, J. Tomasi, *Chem. Phys.* **1981**, *55*, 117–129; b) S. Miertus, J. Tomasi, *Chem. Phys.* **1982**, *65*, 239–245; c) M. Cossi, V. Barone, R. Cammi, J. Tomasi, *Chem. Phys. Lett.* **1996**, *255*, 327–335; d) E. Cancès, B. Mennucci, J. Tomasi, *J. Chem. Phys.* **1997**, *107*, 3032–3041; e) V. Barone, M. Cossi, J. Tomasi, *J. Comput. Chem.* **1998**, *19*, 404–417; f) M. Cossi, G. Scalmani, N. Rega, V. Barone, *J. Chem. Phys.* **2002**, *117*, 43–54.

Received: July 31, 2007

Published Online: November 27, 2007